18 June 1999

ELSEVIER

Chemical Physics Letters 306 (1999) 233–238

CHEMICAL PHYSICS LETTERS

Complete analysis of the Na_3^+ fragmentation in collision with He atoms

M. Barat, J.C. Brenot, H. Dunet, J.A. Fayeton, Y.J. Picard, D. Babikov [1], M. Sizun *

Laboratoire des Collisions Atomiques et Moléculaires Unité Mixte de Recherche C8625, Bâtiment 351, Université Paris-Sud XI, F-91405 Orsay Cedex, France

Received 10 March 1999; in final form 22 April 1999

Abstract

An experimental investigation of the fragmentation mechanisms of Na_3^+ cluster ions in collision with He atoms at 263 eV centre-of-mass energy is presented. The relative populations of the three fragmentation pathways are determined. In particular, the kinematics of the three-body breakup is studied in detail. The analysis of the correlation between the velocity vectors of the fragments allows one to estimate the relative role of the electronic excitation or momentum transfer in the population of each pathway. The discussion of the fragmentation dynamics is based on a concomitant theoretical study.

1. Introduction

Collision-induced dissociation (CID) of metallic clusters provides a means for investigating the dynamics of nuclei and unlocalised electrons after the strong perturbation of a heavy particle collision. At a few 100 eV centre-of-mass energy, the two fragmentation mechanisms, namely *electronic excitation* and *momentum transfer* in binary collisions between projectiles and target atomic cores begin to compete as predicted by the stopping power models [1]. Such a prediction has been recently confirmed [2] by the analysis of the CID of Na_2^+ in an experiment based on a multi-coincident detection of the fragments. Such a simple system with a single active electron has been considered as a prototype for testing various theoretical approaches of the fragmentation process [2,3]. This study has then been extended to small Na_n^+ ($n = 3$–9) clusters in an attempt to disentangle the various fragmentation mechanisms [4]. However, only the dissociation in two fragments could be analysed. In this Letter, we present a complete investigation of the fragmentation pathways including the kinematic analysis of the 3-body dissociation of Na_3^+. The technique of coincidence between 3 fragments has also been recently applied to the study of the coulombic breakup of H_3^+ [5] and to the photo-fragmentation of Ar_4^+ [6]. The present experimental investigation is concomitant with a theoretical investigation of the same subject given in the companion Letter [7] that allows for deeper analysis of the fragmentation dynamics.

2. Experiment

The experimental approach is based on the determination of the velocity vectors of the various frag-

* Corresponding author. E-mail: sizun@lcam.u-psud.fr

[1] Also Moscow Institute of Physics and Technology, Institutsky per. 9, Dolgoproudny, Moscow region, 141700 Russia.

0009-2614/99/$ - see front matter
PII: S0009-2614(99)00448-0

ments detected in coincidence. Briefly [2,4], a mass-selected chopped beam of Na_3^+ ions crosses (at 90°) a cold He target beam produced by a supersonic expansion. The ionic and neutral fragments are separated by an electric field and detected on two position sensitive detectors (PSDs). In all earlier experiments, the neutral fragments arising from 3-body fragmentation are received almost simultaneously on the detector and cannot be identified by the PSD based on the resistive anode technique (3 μs response time during which the PSD is blind to a new particle). Therefore for the present experiment, the neutral PSD has been replaced by a faster one based on a delay line anode [8], resulting in a 20 ns response time. This was achieved at the expense of a slight degradation of the position resolution, 0.3 mm compared to 0.1 mm with the resistive anode. The velocity vectors of all fragments of a given event are obtained from the position and time information. The most significant observables as, e.g., χ the centre-of-mass (CM) scattering angle, Φ the angle between the collision plane (defined by the incident Na_3^+ projectile and the recoiling He target) and the dissociation plane, and ϵ the sum of the kinetic energy of

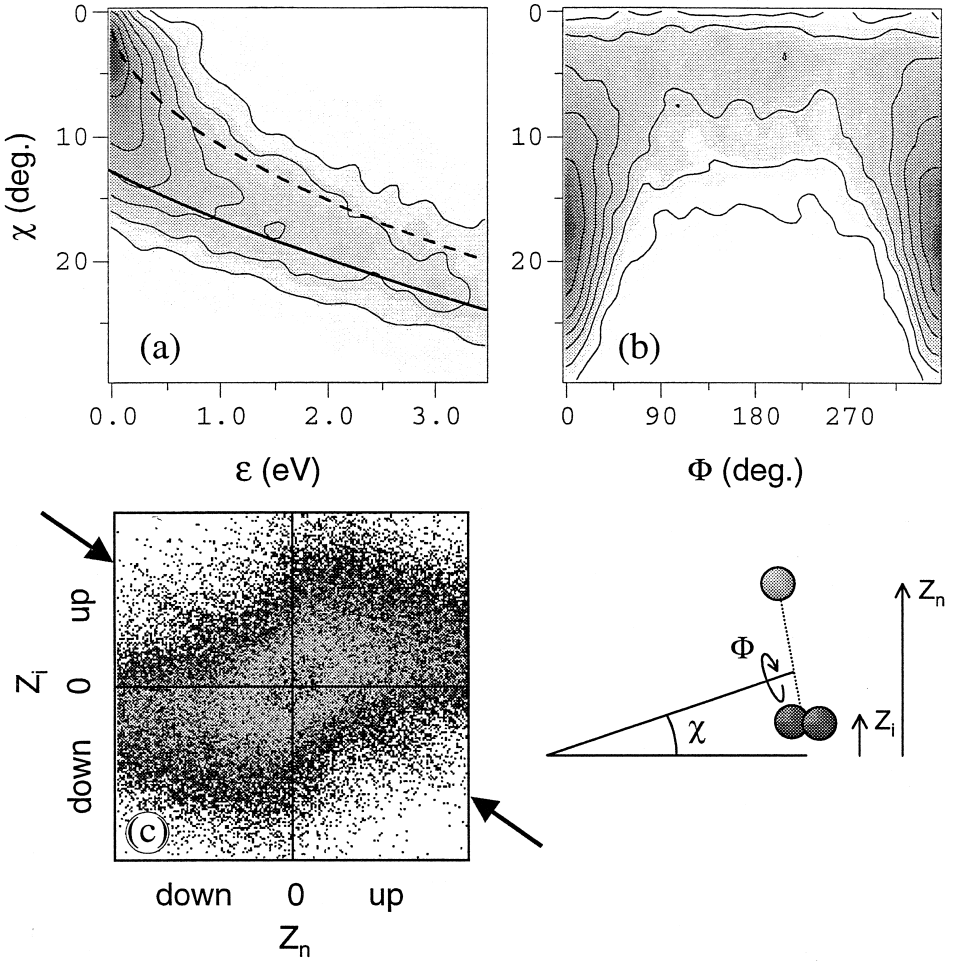

Fig. 1. The $Na_3^+ \rightarrow Na_2^+ + Na$ pathway. (a) $I(\varepsilon, \chi)$ intensity contour map. The full and dashed lines are the predictions of the simple impulsive model, see e.g. Ref. [2], for cold (full line) and vibrationally excited (dashed line) Na_3^+ ions. (b) $I(\Phi, \chi)$ intensity contour map. (c) '*ZZ* correlation' between the impact positions on the detectors of the neutral (Z_n) and ionic fragments (Z_i), see e.g. Refs. [2,4]. The arrows point out the backlash line, a signature of the electronic mechanism: Z_i and Z_n are in opposite directions, indicating a vanishing χ value. The main bulky structure signs the IM2 mechanism.

all fragments in the cluster centre of mass are determined (Fig. 1).

The relative probabilities for the population of the three pathways deduced from the counting rates of the various fragments weighted by the detection efficiencies as discussed in Ref. [4] are given below for a 263 eV centre-of-mass collision energy:

Pathway A	Na_3^+	$\rightarrow Na_2^+ + Na$	90%,
Pathway B		$\rightarrow Na^+ + Na_2$	4%,
Pathway C		$\rightarrow Na^+ + Na + Na$	6%.

The relative Na_2^+ and Na^+ intensity is only dependent on the relative ion detection efficiency and is estimated with a 2% accuracy while the ratio between B and C pathways that is dependent of the absolute neutral detection efficiency is determined with an accuracy not better than 20%.

It will be assumed in this Letter that all fragments are in the electronic ground states, that is only the less endothermal channel of each pathway is populated. The initial vibrational energy of the Na_3^+ ions, unknown experimentally, was arbitrary set to 1 eV in the theory as suggested in some previous work on electron impact ionisation of sodium clusters [9].

3. The $Na_3^+ \rightarrow Na_2^+ + Na$ pathway

Fig. 1a shows the intensity contour diagrams as functions of χ and ϵ. For large scattering angles, the contour lines stretch along the curves given by a model calculation assuming a binary He–Na elastic collision considering a cold (full curve) or a hot, almost dissociated (dashed curve) Na_3^+ ion, respectively. Fig. 1b shows that for large χ values, the dissociation occurs around $\Phi \approx 0°$ as expected for a *direct* impulsive mechanism (IM1) in which a violent He–Na impact results in a direct ejection of a fast Na fragment [2].

A second structure shows up at $\chi < 10°$ and small ϵ values, the analysis of which has been given in Ref. [4]. Actually, this structure corresponds to the sum of two mechanisms.

(i) A *complex* impulsive mechanism (IM2) involves an initial He–Na elastic collision followed by momentum redistribution through Na–Na collisions. In such a mechanism, the dissociation may occur out of the (first) He–Na collision plane giving a wide-spread Φ distribution corresponding to the grey background in Fig. 1b for $\chi < 10°$.

(ii) An electronic mechanism (EM) is responsible for the backslash line in the '*ZZ*' correlation of Fig. 1c. This mechanism also shows up as wiggles around $\chi \approx 3°$, 0.5 eV $< E_{rel} <$ 1 eV in Fig. 1a.

By an adequate filtering of the experimental data, one finds that the relative contributions of the IM1, IM2 and EM mechanisms to the $Na_2^+ + Na$ pathways can be estimated to 55%, 35 %, and 10 %, respectively with an accuracy of $\sim$5%. These values are remarkably close to the theoretical predictions: 60–68%, 23–31%, and 9%, respectively. The contour maps of the two impulsive mechanisms are also well reproduced by the theory, the A1 contribution in Ref. [7]. Notice in particular (Fig. 1a) the stretching of the contours along the χ axis for $\epsilon < 0.5$ eV due to IM2. The EM contribution, A2 in the theoretical analysis [7], is clearly peaked at $\chi \approx 0°$. The disagreement with experiment cannot be considered as significant due to inaccuracies arising in the data processing around $\chi \approx 0°$.

4. The $Na_3^+ \rightarrow Na^+ + Na + Na$ and the $Na_3^+ \rightarrow Na^+ + Na_2$ pathways

Fig. 2a shows the correlation between χ and ϵ the sum of the kinetic energies of the three fragments in the cluster CM frame for the $Na_3^+ \rightarrow Na^+ + Na^+ + Na$ pathway:

(i) A first structure peaked at small χ and ϵ values that accounts for $\sim$40% of the population of that channel is attributed to electronic transitions. This mechanism should primarily correspond to the C3 contribution of the theoretical analysis, a 3-body breakup following an electronic transition towards the 2nd excited potential energy surface (PES). However, the theory predicts too large an energy for ϵ of $\sim$1 eV. This is due to inaccuracy in the calculation of the PES. Indeed a comparison with a full CI calculation shows that the 3rd DIM PES is too repulsive.

(ii) The contour lines extend towards large ϵ values and roughly follow the curves of the binary model indicating mechanisms that involve large momentum transfers. However, in contrast with the previous case, the contours spread out over wider χ

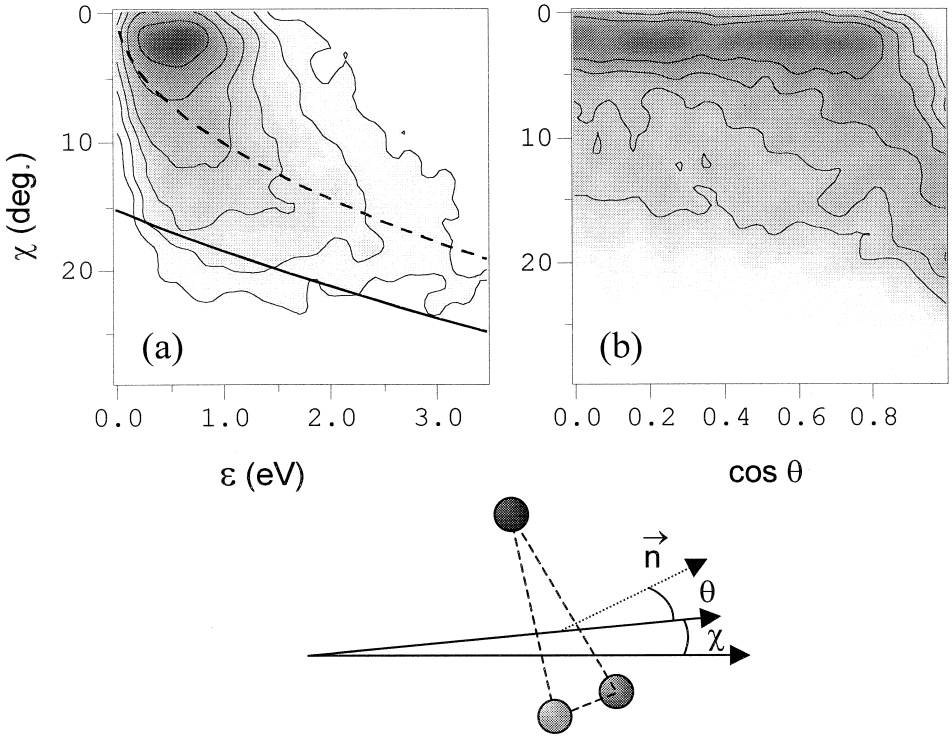

Fig. 2. The $Na_3^+ \rightarrow Na^+ + Na + Na$ pathway. (a) $I(\varepsilon, \chi)$ intensity contour map. The full and dashed lines are the predictions of the simple impulsive model as in Fig. 1. (b) $I(\theta, \chi)$ intensity contour map. θ gives the orientation of the Na_3^+ plane with respect to the scattering axis.

and ϵ ranges. A comparison with the theoretical predictions shows that this wide structure is accounted for by the sum of the C1 and C2 contributions (Fig. 3C of Ref. [7]). Notice that the C1 contribution, which is very sensitive to the cluster internal energy, is overestimated by the theory.

Actually more can be learnt about the 3-body fragmentation dynamics by examining the shape of the dissociating trimer. The $I(\theta, \chi)$ correlation between θ, the angle that defines the orientation of the trimer plane with respect to the scattered axis, and χ the scattering angle (Fig. 2b) shows a distribution isotropic with respect to the trimer plane. Notice that data for $\cos\theta > 0.8$ and small χ are missing. They correspond to a Na_3^+ ion plane parallel to the detector plane. In such cases, the two neutral fragments hit the detector simultaneously (inside the 20 ns dead time) and are not recorded. This is not the case at large χ, at which angle the trimer is skew with respect to the PSD. One can tentatively invoke topological considerations to explain the increase of the contribution (the tail at large χ) of the impulsive mechanisms at large $\cos\theta$.

More insight into the electronic 3-body breakup can be found in the following sets of correlation obtained after filtering the data for $\chi < 5°$. Fig. 3a shows the corresponding data, displayed as a function of the three angles $\hat{n}_1$, $\hat{n}_2$ and $\hat{i}$ defining the Na_3^+ triangle. They clearly exhibit a fragmentation along isosceles geometries with a maximum corresponding to the equilateral triangle, a preferential geometry for fragmentation after electronic excitation on the 3rd PES as predicted by the theory. Fig. 3b displays the correlation between ϵ and the $\hat{n}_1$ angle obtained after selecting isosceles configurations with $\hat{i} \approx \hat{n}_2$ illustrating a dissociation that stretches symmetrically around the equilateral configuration. The same result (not shown here) is obviously obtained for the $I(\epsilon, \hat{n}_2)$ correlation. On the other hand, the $I(\epsilon, \hat{i})$ correlation (Fig. 3c) presents asymmetric contours with a tail extending for small $\hat{i}$ angles towards larger ϵ energies. We suggest that the

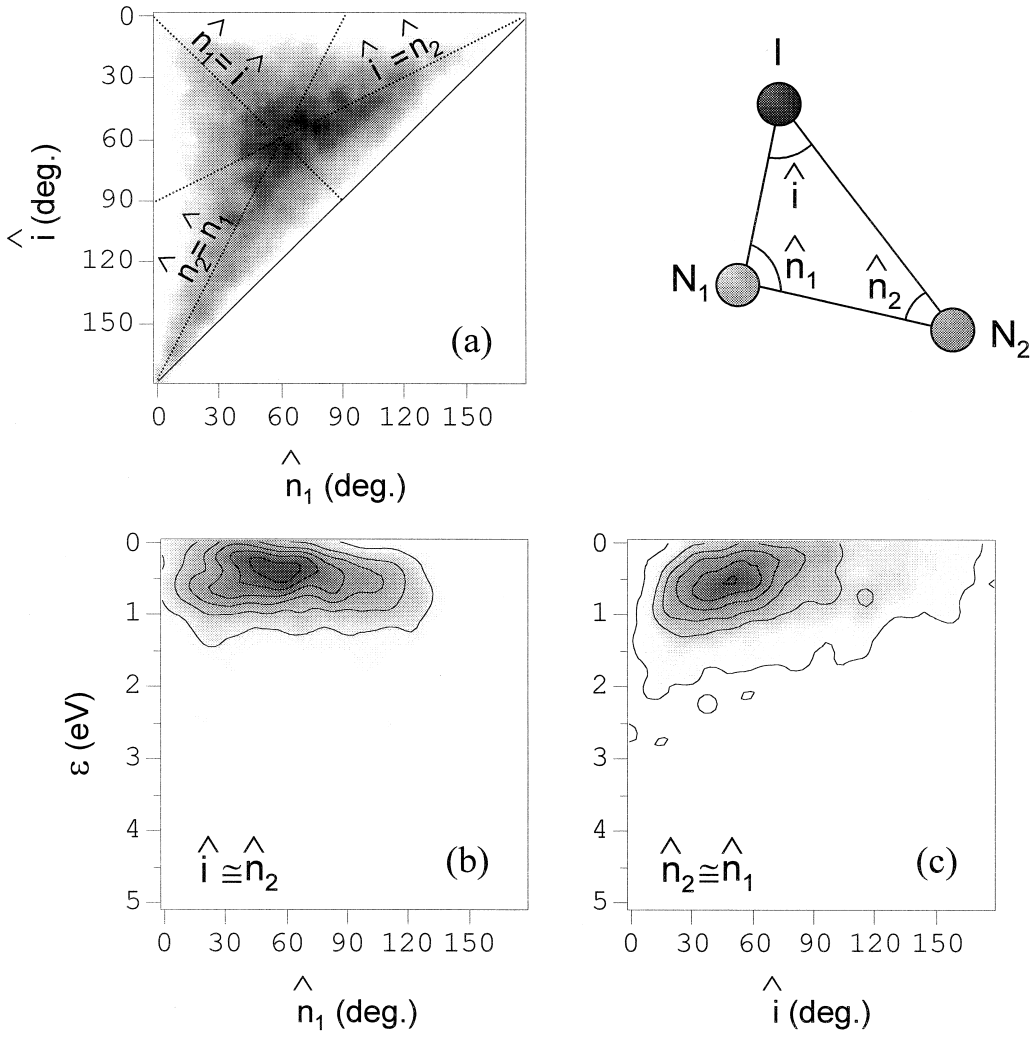

Fig. 3. Shape of the Na_3^+ triangle after dissociation for the forward 3-body breakup ($\chi < 5°$). $\hat{n}_1$, $\hat{n}_2$ and $\hat{i}$ are the angles defining the breakup geometry. (a) $I(\hat{i}, \hat{n}_1)$ angular correlation contour map. (b) and (c) $I(\varepsilon, \hat{n}_1)$ and $I(\varepsilon, \hat{i})$ contour maps, respectively.

$I(\epsilon, \hat{i})$ correlation corresponds to the sum of two contributions: a first one symmetric around 60° similar to the $I(\epsilon, \hat{n}_1)$ correlation superimposed on a second one extending at small $\hat{i}$ angles and large ϵ. This latter configuration $Na_3^+ \rightarrow Na^+ + (Na + Na)$ corresponds to a quasi 2-body dissociation with very small relative velocities between the two Na atoms. This suggests that the mechanism responsible for this fragmentation dynamics corresponds to the C2 contribution in Ref. [7] at small χ. This basic EM might also account, through the B2 contribution, for the $Na_3^+ \rightarrow Na^+ + Na_2$ pathway, a channel that cannot be directly analysed with our technique.

5. Conclusions

The present combined experimental and theoretical study was a first attempt to disentangle the collision-induced fragmentation, including the 3-body breakup, of a triatomic system. The relative roles of electronic and impulsive mechanisms have been established. On the experimental side, efforts will now

be devoted to control better the internal energy of the cluster ions and to extend the range of collision energy. Experimental results [4] are available for the two-fragment dissociation of larger Na_n^+ clusters ($n = 5$–9) that will be completed by multi-fragmentation studies in the near future.

Acknowledgements

The authors wish to thank F. Aguillon and V. Sidis for stimulating discussions and continuous support during this work.

References

[1] J.F. Ziegler, J.P. Biersack, The Stopping and Range of Ions in Solids, Pergamon, New York, 1985.
[2] J.A. Fayeton, M. Barat, J.C. Brenot, H. Dunet, Y.J. Picard, R. Schmidt, U. Saalmann, Phys. Rev. A 57 (1998) 1058.
[3] D. Babikov, F. Aguillon, M. Sizun, V. Sidis, Phys. Rev. A 59 (1999) 330.
[4] M. Barat, J.C. Brenot, H. Dunet, J.A. Fayeton, Y.J. Picard, J. Chem. Phys. 110 (1999) 10758.
[5] L.M. Wiese, O. Yenen, B. Thaden, D.H. Jaecks, Phys. Rev. Lett. 79 (1997) 4982.
[6] P. Jukes, A. Buxey, A.B. Jones, A.J. Stace, J. Chem. Phys. 109 (1998) 5803.
[7] D. Babikov, M. Sizun, F. Aguillon, V. Sidis, Chem Phys. Lett. 306 (1999) 226, (this issue).
[8] O. Jagutzki, V. Mergel, K. Ullmann-Pfleger, L. Spielberger, U. Meyer, R. Dörner, H. Schmidt-Böcking, SPIE Proc. 3438 (1998) (also in: M.R. Descour, S.S. Shen (Eds.), Imaging Spectrometry IV, Proc. SPIE 3438 (1998), p. 322).
[9] L. Bewig, U. Buck, Ch. Mehlmann, M. Winter, J. Chem. Phys. 100 (1994) 2765.